scientific reports

Check for updates

OPEN

# Biosorption of thorium onto *Chlorella Vulgaris* microalgae in aqueous media

Ke Cheng[1], Lingfei Qu[1,2], Zhiqiang Mao[2,3]✉, Rong Liao[2], Yang Wu[3] & Amin Hassanvand[4]✉

**Thorium biosorption by a green microalga, *Chlorella Vulgaris*, was studied in a stirred batch reactor to investigate the effect of initial solution pH, metal ion concentration, biomass dosage, contact time, kinetics, equilibrium and thermodynamics of uptake. The green microalgae showed the highest Th adsorption capacity at 45 °C for the solution with a thorium concentration of 350 mg $L^{-1}$ and initial pH of 4. The amount of uptake raised from 84 to 104 mg $g^{-1}$ as the temperature increased from 15 to 45 °C for an initial metal concentration of 75 mg $L^{-1}$ at pH 4. Transformation Infrared Spectroscopy (FTIR) was employed to characterize the vibrational frequency changes for peaks related to surface functional groups. Also, the scanning electron microscope (SEM) and energy-dispersive X-ray spectroscopy (EDX) were used to determine the morphological changes and elemental analysis of the biosorbent before and after the sorption process. The Langmuir isotherm was in perfect agreement with the equilibrium empirical data of thorium biosorption and the highest sorption capacity of the *Chlorella Vulgaris* microalgae was determined as 185.19 mg $g^{-1}$. Also, the results of kinetic studies show that the thorium biosorption process follows a pseudo-second-order kinetic model. The negative value of $\Delta G^0$ indicates spontaneity and the positive values of $\Delta H^0$ indicate the endothermic nature of the adsorption process.**

**Keywords** Biosorption, Thorium, *Chlorella Vulgaris*, Green microalga, Stirred batch reactor

Radioactive elements with long half-lives and high chemical toxicity that enter the environment through the effluents of various industries have attracted the attention of many researchers to reduce major environmental concerns. One of these radioactive elements is thorium, which can be abundant in uranium and rare earth elements processing sites. Its long half-life is $14.05 \times 10^9$ y[1–3].

Thorium, as a nuclear fuel resource, is about four times more abundant than uranium in the Earth's crust[4–6]. The single isotope Th radionuclide ($^{232}$Th ) is an α – (90%), β – (1%) and γ – (9%) emitter[7–9]. Furthermore, $^{232}$Th is a chemically toxic heavy metal. This toxic radionuclide enters the food chain in even small amounts, it causes serious effects and health problems[10–12]. Considering the biological hazards of this element, it is important to separate and remove it from the wastewater containing it.

Based on a lot of research, it is well known that adsorption can be very helpful for solving environmental pollution problems in wastewater treatment from radionuclides[13–15]. Various types of biological, polymeric and natural sorbents have been researched and investigated for the sorption and separation of thorium from wastewater and solution media[16–20].

These researches prove that microorganisms such as fungi, yeast, bacteria and algae are capable of uptake of thorium from wastewaters higher than 15% of biosorbent dry weight[20,21]. Such a metal loading capacity (higher than 15% of biosorbent dry weight) has been identified as an economic threshold for the use of biosorption technology compared to other methods such as reverse osmosis, precipitation, and liquid-liquid extraction[22–24].

Algal biomass, including microalgae, macroalgae, and cyanobacteria, has distinct advantages over other microbial biomass due to the wide range of morphological types available, large-scale availability, products derived from industrial processes, and fermentation. Several algal biomasses have been widely used for the biosorption of heavy metal ions and radionuclides. Thorium uptake has also been reported using different algal biomass, for example, Cystoseira, *Sargassum*, *Ulva*, *Palmaria elegans*, and *Chondrus crispus*[25–28].

[1]Sichuan Development Environmental Science and technology Research Institute Co., Ltd, Chengdu 610041, Sichuan, China. [2]Chengdu University of Technology, Chengdu 610059, Sichuan, China. [3]Sichuan Tianshengyuan Environmental Services Co., Ltd, Chengdu 610036, Sichuan, China. [4]Department of Polymer Engineering, Faculty of Engineering, Lorestan University, Khorramabad, Iran. ✉email: 18000590611@163.com; hasanvand.a@lu.ac.ir; amin.hassanvand1361@gmail.com

The green microalgae *Chlorella vulgaris* has shown satisfactory sorption and removal of heavy metals and radionuclides such as uranium, strontium, copper, zinc, cadmium and nickel from aqueous solutions[29–33]. This work focused on the investigation of thorium biosorption using *Chlorella vulgaris*, a green microalgae biomass. Despite the high abilities of the biosorbent *Chlorella vulgaris* to adsorb heavy metals, no extensive study has been done for the adsorption of thorium.The sorption capacity of *Chlorella vulgaris* for sorption of thorium from aqueous media in batch experiments at different operating conditions was studied. Kinetic and isotherm models were employed to determine the optimum sorption dynamic and equilibrium models. In addition, in order to discuss on biosorption mechanism of thorium by microalgae biomass, the thermodynamic aspects of the process were studied and evaluated.

## Materials and methods

### Cells and growth conditions

The unicellular green microalgae *Chlorella vulgaris* was obtained from the Caspian Sea Ecology Research Center. *Chlorella vulgaris* cells were grown at 25 °C in Erlenmeyer flasks containing Zarouk's standard solution media[34]. The light intensity of 3500 lx was used to illumine the Erlenmeyer surface. An air pump (RESUN AC-9603) was used for aeration with a pressure of 0.12 MPa. Using deionized distilled water, the cultured cultivated algae were washed to eliminate the mediators. The obtained microorganism was centrifuged at 4000 rpm for 35 min. The microalgae were then dehydrated in an oven at 100 °C for 60 min and so were stored for further biosorption experiments.

### Chemicals and solutions

In order to prepare thorium solutions with different concentrations, first a mother solution with a concentration of 1000 mg $l^{-1}$ was prepared using thorium nitrate salt ($Th(NO_3)_4{\cdot}6H_2O$), analytical grade, in pure distilled water. Then the target solutions for tests were made by careful dilution from the mother solution. Also, sodium hydroxide 1 M and nitric acid 1 M were used for pH adjustments of the solutions. All chemicals and reagents used were analytical grades and obtained from Sigma-Aldrich, Germany.

### Instruments

An inductively coupled plasma atomic emission spectrometer, ICP-AES model 7300 DV USA, was used to analyze thorium concentration in solutions. A pH meter (744 Metrohm Herisau, Switzerland) was employed to evaluate the pH values of the solutions. A shaker incubator was used in the batch sorption tests. A scanning electron microscopy, SEM Hitachi S-4160 Japan, was employed to analyze the morphology of the biosorbent. Fourier transform infrared spectroscopy (FTIR), Bruker Optik GmbH, model IFS 88 Germany, was used to characterize the biosorbent in the range of 400–4000 $cm^{-1}$. Energy-dispersive X-ray spectroscopy (EDX), JEOL JEM-2100 Japan, was used to elemental analysis of the biomass before and after biosorption.

### Batch sorption procedure

Biosorption experiments were accomplished in a batch system to study the influence of effecting parameters such as initial pH of the solution, contact time, biosorbent dosage and operating temperature on the sorption of thorium ions from aqueous solutions. First, the adsorption equilibrium time should be determined through kinetic experiments; For this purpose, 0.5 ml samples of the solution under adsorption were taken at certain time intervals and were set aside for concentration analysis by the ICP-AES after proper dilution. Adsorption equilibrium test was performed on a shaking incubator so that a certain amount of biomass was mixed with a predetermined amount of thorium solution and stirred at 150 rpm for the obtained equilibrium time. This was done at different temperatures.

The initial pH of the solution was adjusted by NaOH solution and, if necessary, nitric acid solution was also used. After sorption, a Whatman filter paper (No. 42) was used to filter the solution before concentration analysis by ICP-AES. The amount of equilibrium uptake of thorium ions, $q_e$ (mg $g^{-1}$), and removal percentage, were obtained as follows, respectively:

$$q_e = \frac{C_i - C_e}{M} \times V \tag{1}$$

$$R\% = \frac{C_i - C_e}{C_i} \times 100 \tag{2}$$

where $C_i$ and $C_e$ are the initial and the equilibrium concentrations of metal ions in the solution phase (mg $L^{-1}$), V is the volume of solution (L) and M is the adsorbent dosage (g). All tests were completed in triplicate. The arithmetic average was reported as experimental data.

### Sorption isotherms

Sorption isotherm models are essential for the design of any biosorption system. Several models have been developed and applied to model the behavior of biosorption systems under equilibrium conditions. The important and practical models for biosorption systems are Freundlich, Langmuir, Redlich–Patterson, Dubinin–Radushkevich and Temkin isotherm models, which have been evaluated to fit the equilibrium data of many sorption systems. The models used to fit the equilibrium data of thorium biosorption with *Chlorella vulgaris* are Freundlich, Langmuir, Temkin and Dubinin–Radushkevich, expressed by Eqs. (3)–(6), respectively.

$$q_{eq} = K_F C_e^{\frac{1}{n}} \tag{3}$$

where $K_F$ [(mg $g^{-1}$) (L $mg^{-1})^{1/n}$] and 1/n and refer to the sorption capacity and intensity of sorption, respectively. The sorption is favorable when n stays between 1 and 10.

$$\boldsymbol{q_{eq}} = \frac{q_{max}\boldsymbol{bC_{eq}}}{1 + \boldsymbol{bC_{eq}}} \tag{4}$$

where $q_{max}$ is the maximum sorption capacity of the biosorbent (mg $g^{-1}$) and b is the Langmuir constant (L $mg^{-1}$). The Langmuir isotherm is based on the formation a complete monolayer on the surface of binding cells at high $C_{eq}$. The constant b in Langmuir isotherm represents the affinity of binding sites.

$$q_{eq} = \frac{RT}{b_T}\ln(A_T C_e) \tag{5}$$

where $A_T$ (L $mg^{-1}$) is related to the equilibrium binding, T is the absolute temperature in K, R is the universal gas constant (8.314 J $mol^{-1}$ $K^{-1}$), and $b_T$ is related to sorption heat.

$$q_{eq} = q_{max}.e^{-k\varepsilon^2} \tag{6}$$

where $q_{max}$ is the maximum theoretical sorption capacity of the biosorbent (mg $g^{-1}$), k ($mol^2$ $kJ^{-2}$) is Dubinin–Radushkevich constant. The parameter $\varepsilon$ is Polanyi potential and is equal to,

$$\varepsilon = RTln(1 + \frac{1}{C_e}) \tag{7}$$

The mean sorption energy, E (kJ $mol^{-1}$) is calculated with Eq. (8) using D–R constant, k. The range of energy of sorption at 2–20 kJ $mol^{-1}$ is physisorption.

$$E = \frac{k^{-\frac{1}{2}}}{\sqrt{2}} \tag{8}$$

## Sorption kinetics

In a well-stirred biosorption system, the influence of the external film diffusion on the adsorption rate can be assumed to be negligible, so the measured adsorption data will be proportional to the cell surface concentration; The Lagergren's pseudo-first-order and Ho's pseudo-second-order models mainly used to describe the dynamic behavior of such biosorption systems; The pseudo-first- and -second-order models are described by the Eqs. (9) and (10), respectively.

$$\frac{dq_t}{dt} = k_1(q_e - q_t) \tag{9}$$

$$\frac{dq_t}{dt} = k_2(q_e - q_t)^2 \tag{10}$$

where $q_t$ is the mass of adsorbed thorium ion per unit mass of dried biomass at time t, $k_1$ is the rate constant of first order and $k_2$ is the rate constant of second order biosorption.

An adsorption process involves the transport of the adsorbate from the bulk solution to the inner surface of the pores of adsorbent. The intraparticle diffusion step may become the rate controlling factor for an adsorption process. Weber and Morris theorized that the rate of intraparticle diffusion varies proportionally with the half power of time and is expressed as[35–37]:

$$q_t = K_{id}t^{0.5} + C \tag{11}$$

where $q_t$ is the metal biosorbed at time t, in mg $g^{-1}$, t is the contact time, in min, and $K_{id}$ is the intraparticle diffusion rate constant, in mg/g $min^{0.5}$. According to Weber and Morris, if the rate limiting step is intraparticle diffusion, a plot of solute adsorbed against the square root of the contact time should yield a straight line passing through the origin[36]. In Weber and Morris the C value is related to the boundary layer thickness, i.e., the larger the value of the intercept, the greater is the boundary layer effect[36].

## Sorption thermodynamic

The biosorption of heavy metal ions and radionuclides can be expressed as a reversible heterogeneous equilibrium process as follows:

radionuclide in aqueous solution ↔ radionuclide-biosorbent.

The thermodynamic assessment of a biosorption process is required to evaluate the spontaneity of the process. The Gibbs free energy change, $\Delta G^0$, is a criterion of the spontaneity of a chemical reaction. Thermodynamic

parameters including the change in free energy ($\Delta G^0$), enthalpy ($\Delta H^0$) and entropy ($\Delta S^0$) were calculated for the system by:

$$\ln K_c^\circ = \frac{\Delta S^0}{R} - \frac{\Delta H^0}{RT} \tag{12}$$

where $K_c^o$ is the standard thermodynamic equilibrium constant. The $K_c^o$ constant is related to the Gibbs free energy by the following relationship:

$$\Delta G^0 = -RT \ln K_c^\circ \tag{13}$$

The equilibrium constant, $K_c^o$, is defined as:

$$K_c^0 = \frac{C_{ad,eq}}{C_{eq}} \tag{14}$$

where $C_{ad,eq}$ is the concentration of metal ion on the adsorbent at equilibrium and $C_{eq}$ is equilibrium concentration of metal ion in solution.

## Results and discussion

### Biosorption characterization

The biosorbents were characterized using Brunauer-Emmett-Teller (BET) analysis, FTIR spectra, SEM micrograph techniques and EDX analyses to recognize the surface morphology. FTIR has been largely employed to obtain information on active functional groups in biomass specimens. The functional groups may be included O–H, N–H, C=O, =C–H, –CH2, –CH3, C–O–C, and > P=O on the surface cells of biosorbents[38]. Figure 1 shows the FTIR spectra of chlorella vulgaris microalgae at a scanning region of 4000–400 $cm^{-1}$. The main peak of 3387 $cm^{-1}$ in the region of about 3000–3600 $cm^{-1}$ is related to O–H stretching and N-H stretching, amide functional group indicating the presence of amide bonds mainly C=O stretching (amide I) at the wave number of 1657 $cm^{-1}$ and a combination of N–H and C–H stretching vibrations 1536 $cm^{-1}$ (amide II) in Protein or other compounds of the cell wall of algae[39]. The carbohydrate –O–C stretching of polysaccharides was characterized by vibrations at 1080 $cm^{-1}$ and C–O–C bending of polysaccharides at 1048 $cm^{-1}$[38]. The main peak at 1422 $cm^{-1}$ indicates the bending of methyl groups on the microalgae. The carboxylic acid group bending in the algae was characterized by vibrations at a peak of 1242 $cm^{-1}$[40].

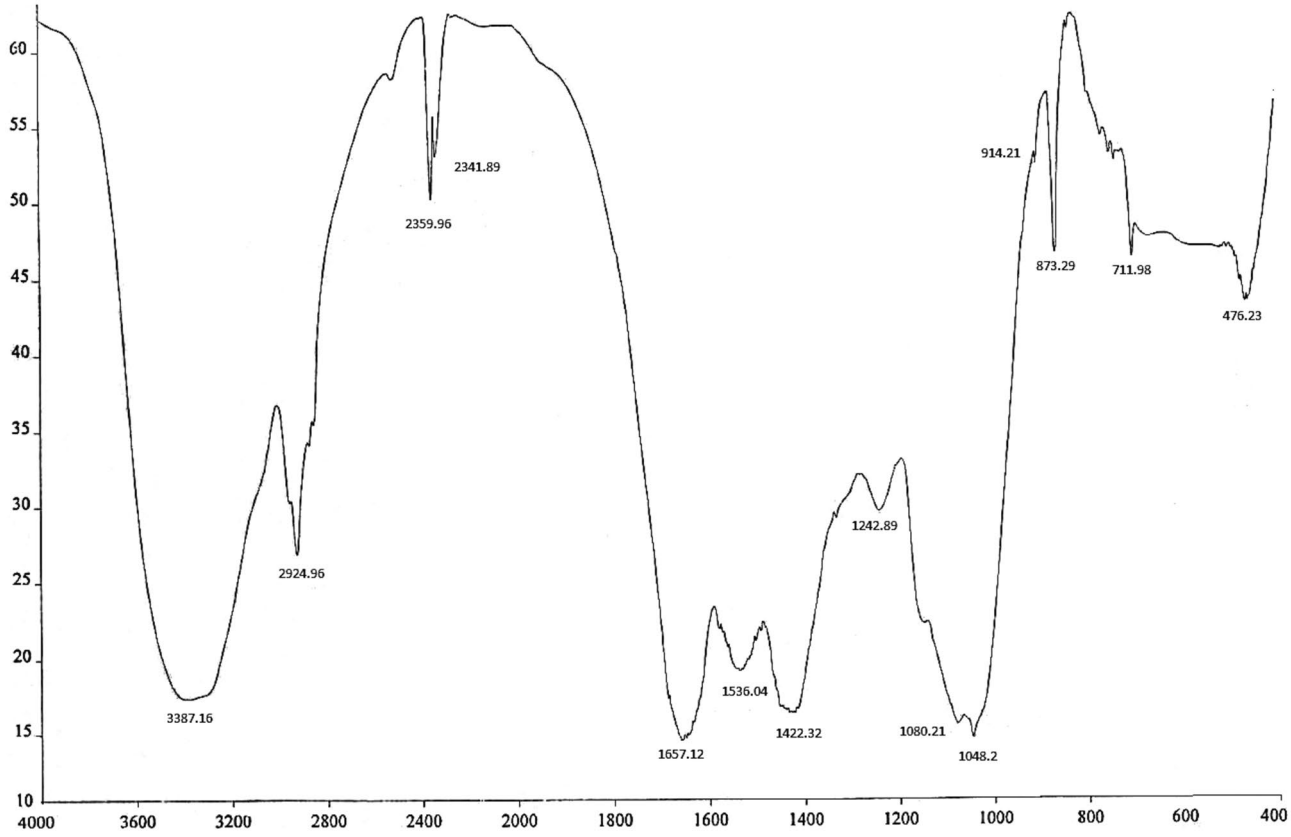


**Fig. 1.** FTIR spectra of the microalga of *Chlorella vulgaris*.

The surface area and the pore volume of *Chlorella vulgaris* green microalgae samples were determined by a porosimeter and surface area analyzer, BELSORP-max instrument, model BEL, Japan, using $N_2$ as adsorbate. Using BET analysis, the surface area and pore volume were determined as 12.8 $m^2 g^{-1}$ and 0.0102 ml $g^{-1}$, respectively.

The surface structure of biomass samples was studied using the scanning electron microscopy technique. The surface structure of the Chlorella vulgaris biosorbent before and after Th adsorption was shown in Fig. 2a,b, respectively; which showed clear changes between before and after the absorption process. As can be seen from Fig. 2a, there are many small grooves on the surface of the biomass but their prominence has decreased after adsorption (Fig. 2b). The morphological changes that occur, may be due to the exposure of thorium ions to microalgae cells; which indicates the successful uptake of thorium in the biomass. Also, elemental analysis was carried out using Energy-dispersive X-ray spectroscopy (EDX) before and after biosorption for confirmation of the adsorption process of thorium on the adsorbent. In a comparison of the EDX analyses of *chlorella vulgaris* before and after thorium ions biosorption (Fig. 3a,b), significant alterations were found along with the appearance of Th peak, demonstrating the attachment of Th on the algae biomass of *chlorella vulgaris*.

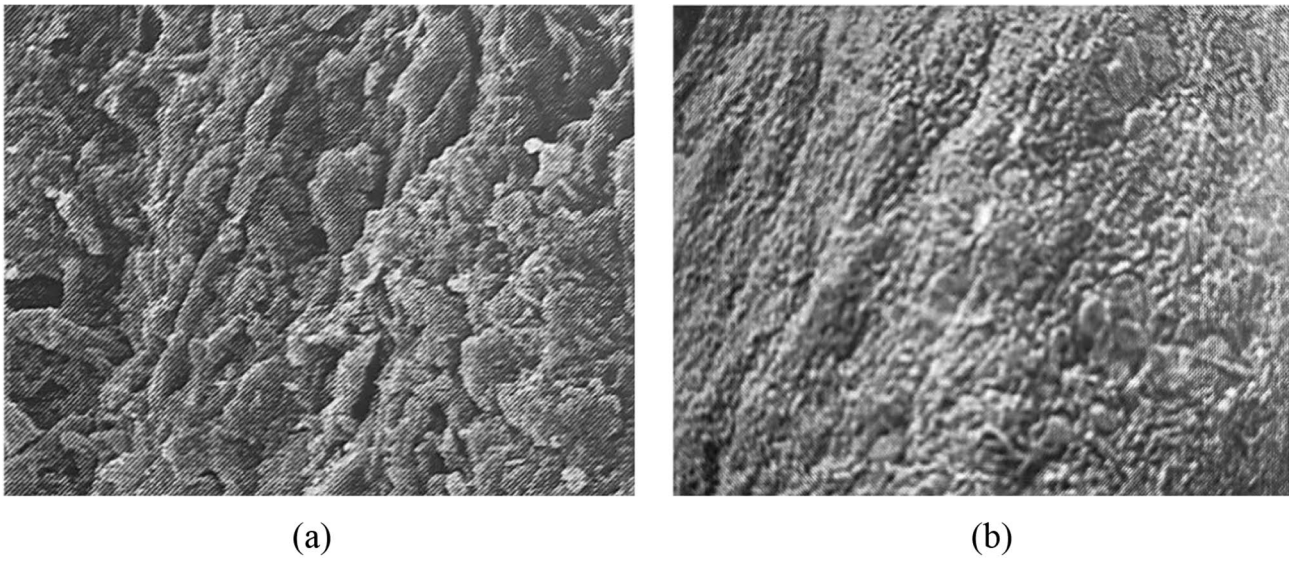


**Fig. 2.** SEM images of surface structure of *Chlorella vulgaris* biomass before (**a**) and after Th adsorption (**b**).

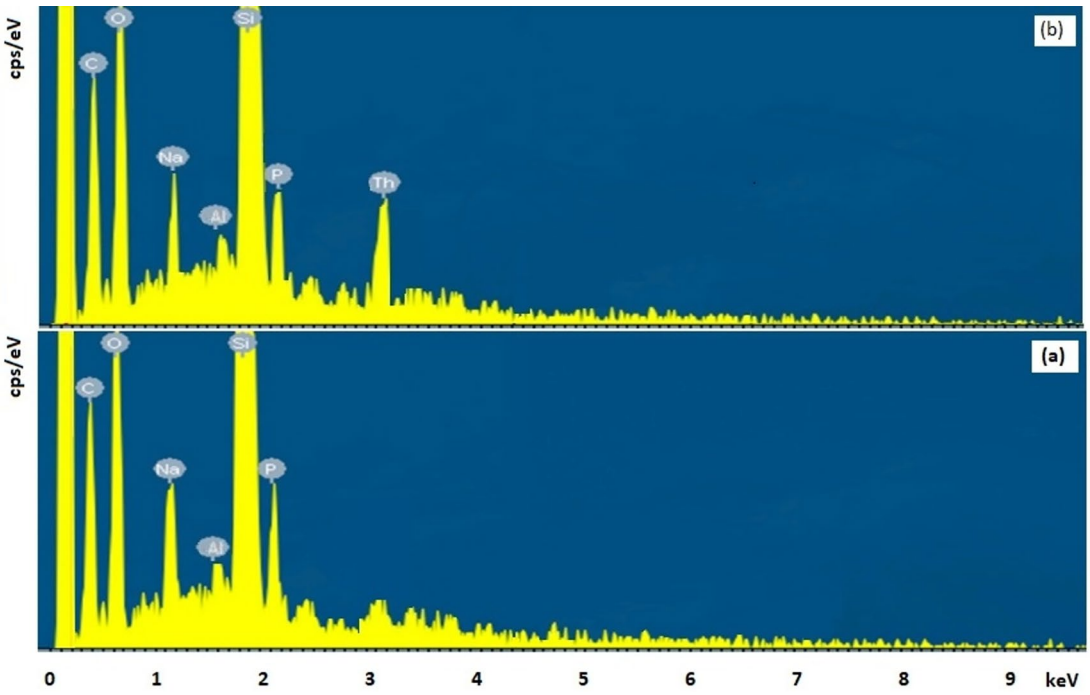


**Fig. 3.** EDX images of of *Chlorella vulgaris* biomass before (**a**) and after Th adsorption (**b**).

## Effect of pH

The pH of the solution is a parameter that can affect the surface charge of the adsorbent and the ionization of the metal ions present in the solution. At pH 2.0, the solubility of thorium is very high and exists as $Th^{4+}$. However, with increasing pH, thorium hydrolysis shifts the solution chemistry toward the formation of the hydrolyzed species $Th(OH)_2^{2+}$, $Th(OH)^{3+}$, $Th_2(OH)_2^{6+}$ and $Th_6(OH)_{15}^{9+}$[41].

To investigate the influence of the initial pH of solution on Th sorption by *Chlorella vulgaris* microalgae, 0.05 g of biosorbent was mixed with 100 ml of 75 mg $l^{-1}$ thorium solution at different pH values in the range of 2–7 for 12 h at 25 °C. As can be seen in Fig. 4. the maximum thorium uptake at equilibrium occurred at pH 4.0. At low pHs, the acidity of the solution is high and there is a competition between thorium ions and $H^+$ ions to be sorbed on the biosorbent. With increasing pH the predominant hydrolyzed species favor the biosorption process, the hydrolyzed species $Th(OH)_2^{2+}$, $Th(OH)^{3+}$, $Th_2(OH)_2^{6+}$ and $Th_6(OH)_{15}^{9+}$ being more efficiently biosorbed than $Th^{4+}$[42]. At much higher pHs, the hydrolysis reaction of metals favors the formation of complexes with a higher positive charge, $Th_2(OH)_2^{6+}$, $Th_3(OH)_5^{7+}$ and $Th_4(OH)_8^{8+}$ complexes, which is difficult to adsorb into binding sites and leads to a decrease in biosorption[20].

## Effect of biosorbent dosage

The effect of the adsorbent dose on the absorption of thorium on the biomass of *Chlorella vulgaris* and its removal from the solution, under the operating conditions of the initial thorium concentration of 75 mg $L^{-1}$, pH 4 and temperature 25 °C, can be seen in Fig. 5. The removal increases from 15 to 97% with increasing adsorbent dose, because the higher the biomass dose in solution, the more available adsorption sites for ions. However, the

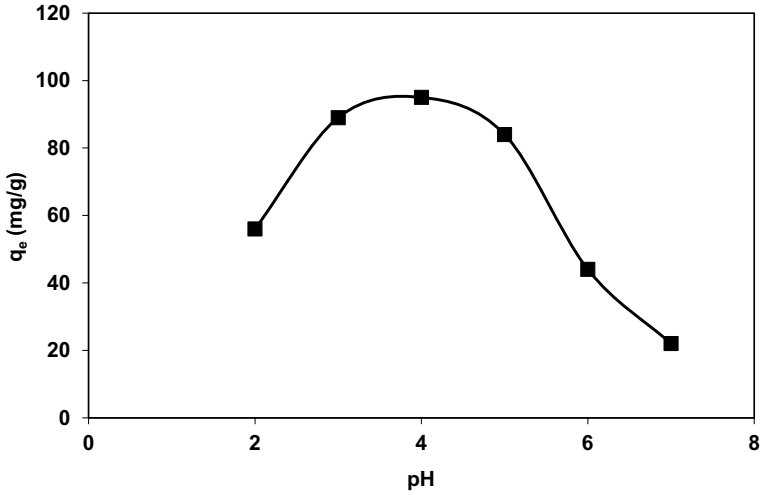


**Fig. 4.** Influence of initial pH of solution on thorium biosorption by *Chlorella vulgaris* (initial thorium concentration 75 mg $L^{-1}$, biomass dosage 0.5 g $L^{-1}$, temperature 25 °C and contact time 12 h).

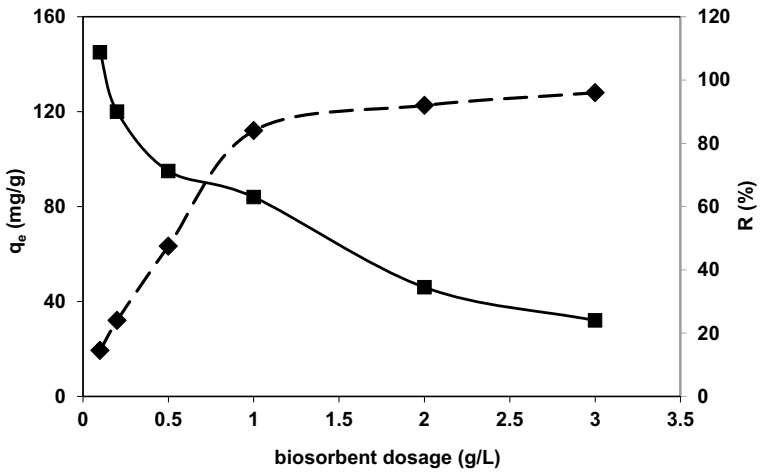


**Fig. 5.** Effect of biomass dosage on thorium biosorption by *Chlorella vulgaris*.

equilibrium adsorption rate of thorium decreases with the increase of biomass dose. This decrease occurred due to the decrease in the availability of adsorbed ions for the unit amount of biomass.

## Effect of contact time and kinetic studies

The effect of contact time on the adsorption process is shown in Fig. 6. As can be seen, the general trend indicates the dual-phase nature of the adsorption process. So that the initial rapid absorption occurred within 30 min of contact time and continued to decrease later to reach equilibrium after about 2 h of contact time.

The pseudo-second-order kinetic and pseudo-first-order models were used to fit the kinetic data and plots of t/q and log ($q_e - q$) versus t (Figs. 7 and 8, respectively). The equilibrium uptake and rate constant calculated from the slope and intercept of the pseudo-first-order and pseudo-second-order plots are tabulated in Table 1. The data presented in Table 1 obtained from the modeling of adsorption kinetics with pseudo-first and second-order equations show excellent fit with the pseudo-second-order model ($R^2$ value > 0.99). This is further confirmed by comparing the calculated $q_e$ obtained from the pseudo-second-order model with the experimental $q_e$, which showed a very good fit between the experimental data and the predicted data obtained from the adsorption model curve.

In order to evaluate the intraparticle diffusion effect in kinetics of thorium adsorption by *chlorella vulgaris*, the line of $q_t$ versus $t^{0.5}$ was plotted (Fig. 9). It can be seen from the figure that the fitting results are not satisfactory (very low $R^2$ value) and also the line didn't pass through the origin. Hence, in this case, intraparticle diffusion

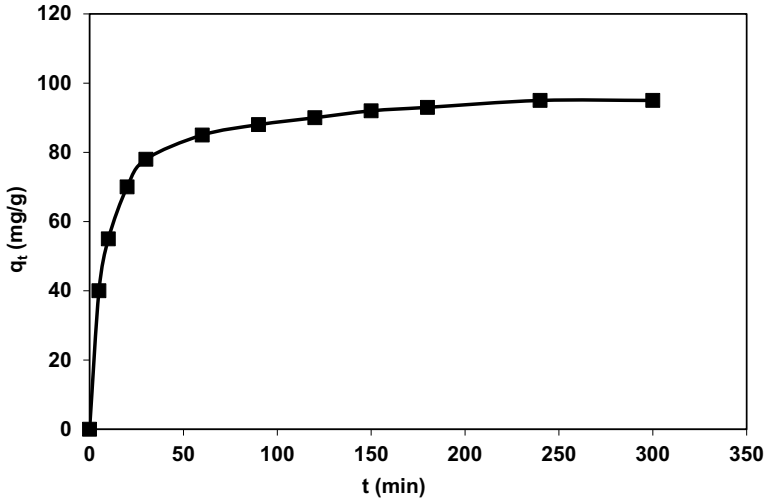


**Fig. 6.** Effect of contact time on thorium biosorption by *Chlorella vulgaris* (initial thorium concentration 75 mg $L^{-1}$, pH 4, biomass dosage 0.5 g $L^{-1}$ and temperature 25 °C).

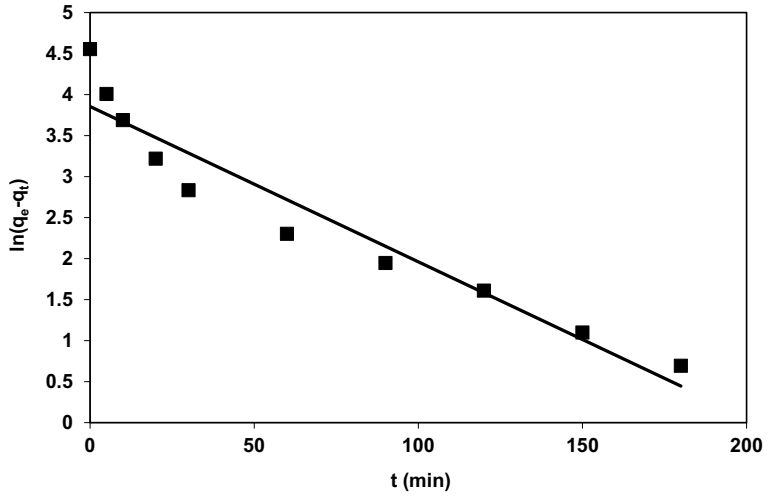


**Fig. 7.** Pseudo-first-order kinetics of thorium biosorption by *Chlorella vulgaris* at initial thorium concentration of 75 mg $L^{-1}$ pH of 4, biomass dosage of 0.5 g $L^{-1}$ and 25 °C.

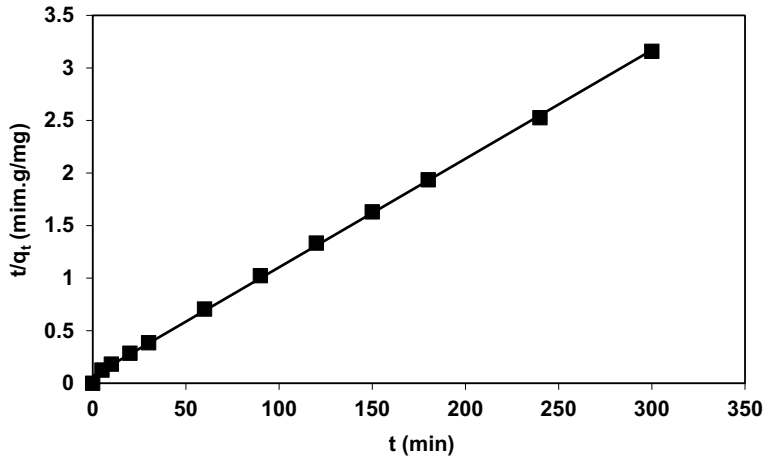


**Fig. 8.** Pseudo-second-order kinetics of thorium biosorption by *Chlorella vulgaris* at initial thorium concentration of 75 mg $L^{-1}$ initial thorium concentration of 75 mg $L^{-1}$ pH of 4, biomass dosage of 0.5 g $L^{-1}$ and 25 °C. pH of 4, biomass dosage of 0.5 g $L^{-1}$ and 25 °C.

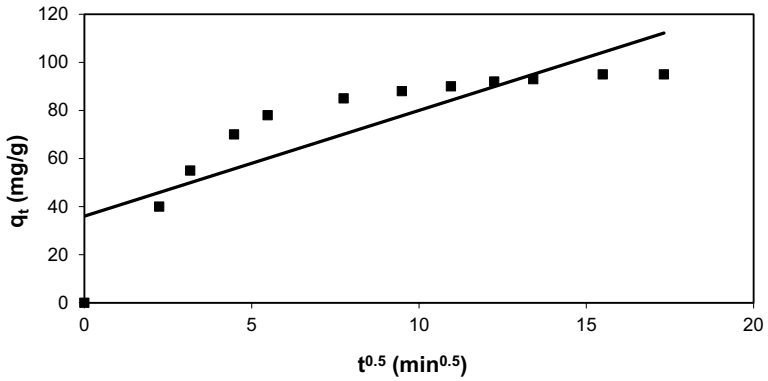


**Fig. 9.** Weber and Morris model for thorium biosorption by *Chlorella vulgaris* at initial thorium concentration of 75 mg $L^{-1}$ pH of 4, biomass dosage of 0.5 g $L^{-1}$ and 25 °C.

| Kinetic model | Parameters | Value |
|---|---|---|
| Lagergren's pseudo-first-order | $k_1$ ($min^{-1}$) | $1.89 \times 10^{-2}$ |
| | $q_e$ (mg $g^{-1}$) | 47.2 |
| | $R^2$ | 0.9253 |
| Ho's pseudo-second-order | $K_2$ (g $mg^{-1}$ $min^{-1}$) | $1.513 \times 10^{-3}$ |
| | $q_e$ (mg $g^{-1}$) | 97.08 |
| | $R^2$ | 0.9994 |
| Weber and Morris intraparticle diffusion | $k_{id}$ (mg $g^{-1}$ $min^{-0.5}$) | 4.3964 |
| | C (mg $g^{-1}$) | 36.04 |
| | $R^2$ | 0.7127 |

**Table 1.** Kinetics parameters for thorium ions biosorption by *Chlorella vulgaris*.

is not the only rate-limiting step. The rate constants calculated from the slope and intercept of the Weber and Morris intraparticle diffusion model are presented in Table 1.

## Biosorption isotherms, effect of adsorbate concentration

The initial concentration of adsorbate in solution provides the main driving force for the transfer of metal ions between the aqueous and solid phases in a biosorption system. Thus, the higher the initial concentration, the

faster and easier the adsorption. However, considering that most of the pollutants in real effluents are in low concentrations, the adsorption process should be evaluated in the range of concentrations close to reality.

Figure 10 shows the effect of initial thorium ion concentration on the adsorption process at an initial solution pH of 4, biomass dosage of 0.5 g $L^{-1}$ and 25 °C; As the initial metal ion concentration increases, thorium adsorption increases due to the increase in the mass potential difference between the solution and the adsorbent. But at metal ion concentrations above a certain limit, due to the limited number of surface binding sites on the cells, adsorption reaches a saturation state and then no significant increase is observed.

The adsorption isotherm models were studied by using the equilibrium experimental data obtained at pH 4, temperature 25 °C and biosorbent dosage 0.5 g $L^{-1}$. The data were fitted using the linear forms of Eqs. (3)–(6). The respective intercepts and slopes represent the constants of the isotherms from their linear graphs. The calculation values for constants of each isotherm along with their fitting correlation coefficients ($R^2$) are presented in Table 2. The comparison of regression correlation coefficients for different isotherms shows that the Langmuir model with the highest regression correlation coefficient ($R^2 > 0.99$) has the best match with the thorium sorption process by *Chlorella vulgaris*.

According to the Langmuir isotherm, there is a homogeneous surface consisting of only one layer that has contributed to the adsorption of ions. The graph obtained by modeling the equilibrium data using the Langmuir linear form is presented in Fig. 11. The parameter $q_{max}$ (maximum capacity) calculated from the Langmuir model determines the total capacity of the *Chlorella vulgaris* biosorbent for thorium. A higher value of b also indicates a strong affinity of thorium to adsorb with *Chlorella vulgaris*.

As shown in Table 2, the maximum capacity of the *Chlorella vulgaris* biosorbent for thorium biosorption based on Langmuir isotherm is 185.19 mg $g^{-1}$. So, it can be an effective biosorbent in thorium biosorption from wastewaters. In order to comparison, the maximum sorption capacities of some biological adsorbents for removal of thorium, reported in literature, are given in Table 3.

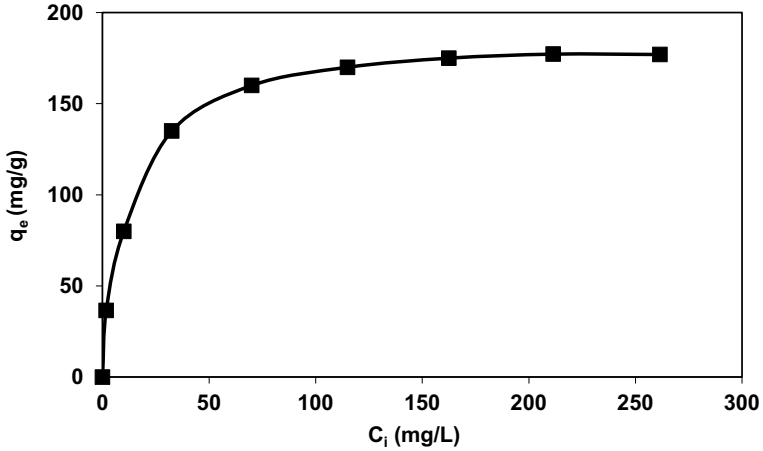


**Fig. 10.** Effect of initial thorium concentration in solution on thorium biosorption by *Chlorella vulgaris* at biomass dosage of 0.5 mg $L^{-1}$ pH of 4, temperature of 25 °C.

| Isotherm model | Parameters | Value |
|---|---|---|
| Langmuir | b (L $mg^{-1}$) | $9.51 \times 10^{-3}$ |
| | $q_{max}$ (mg $g^{-1}$) | 185.19 |
| | $R^2$ | 0.9996 |
| Freundlich | $K_F$ [(mg $g^{-1}$) (L $mg^{-1})^{1/n}$] | 36.29 |
| | n | 3.17 |
| | $R^2$ | 0.9357 |
| Dubinin–Radushkevich | $K_{D-R}$ ($mol^2$ $J^{-2}$) | 47.87 |
| | $q_m$ (mg. $g^{-1}$) | 175.54 |
| | $R^2$ | 0.9684 |
| Temkin | $K_T$ (L $mg^{-1}$) | 1.99 |
| | $b_T$ (J $mol^{-1}$) | 82.27 |
| | $R^2$ | 0.9738 |

**Table 2.** Isotherm parameters for thorium ions biosorption by *Chlorella vulgaris*.

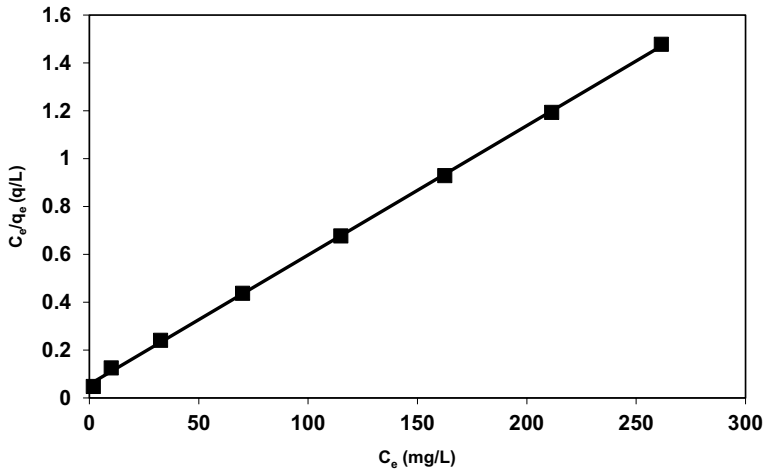


**Fig. 11.** The linearized Langmuir isotherm of thorium biosorption by *Chlorella vulgaris*.

| Sorbent material | $q_{max}$ (mg $g^{-1}$) | References |
|---|---|---|
| *Ginkgo leaf* | 103.8 | [43] |
| *Giant Kelp biomass* | 135 | [44] |
| *Cystoseira indica* | 169.49 | [20] |
| Aspergillus fumigatus | 370 | [19] |
| *Orange peel* | 87.7 | [45] |
| *Cellulosimicrobium cellulans* | 220.56 | [46] |
| *Sargassum aquifolium* | 24.1 | [47] |
| *fungus Fusarium sp.* | 11.35 | [48] |
| *Padina* sp., algae biomass | 185.19 | Present work |

**Table 3.** Comparison of adsorption uptake of various biosorbent for thorium removal from aqueous solutions.

## Biosorption thermodynamics, the effect of temperature

In biosorption processes, another parameter that can affect the amount of initial sorption rate and also equilibrium metal uptake is temperature. Experimental data for the thorium adsorption process by Chlorella vulgaris show that sorption capacity increases with temperature change from 15 to 45 °C (Fig. 12).

Thermodynamic parameters of biosorption, standard enthalpy and entropy changes can be determined from the plot of ln $K_c$ vs. 1/T. The $K_c$, distribution coefficient, was evaluated from the $C_{ad}/C_e$ for different temperatures.

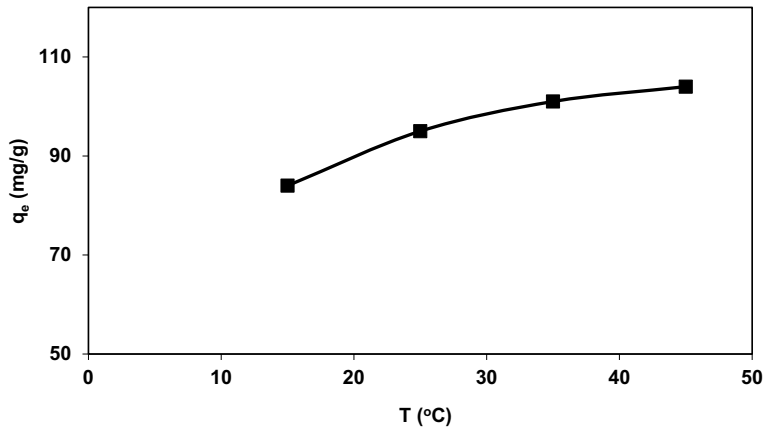


**Fig. 12.** Effect of temperature on thorium biosorption by *Chlorella vulgaris* at biomass dosage of 0.5 mg $L^{-1}$ and pH of 4 for solution with 75 mg $g^{-1}$ initial thorium concentration.

| Temperature | ΔG (kJ mol$^{-1}$) | ΔH (kJ mol$^{-1}$) | ΔS (kJ mol$^{-1}$ K) |
|---|---|---|---|
| 288 | 6.6 | 13.598 | 0.0703 |
| 298 | 7.5 | | |
| 308 | 8.0 | | |
| 318 | 8.8 | | |

**Table 4.** Thermodynamic parameters for thorium biosorption by *Chlorella vulgaris*.

$K_c$ is related to the standard Gibbs free energy according to Eq. (13). Based on this, the information related to biosorption thermodynamic parameters, enthalpy and entropy changes and Gibbs free energy have been calculated and presented in Table 4. The negative value of $\Delta G^0$ is due to the fact that the biosorption of thorium ions into chlorella vulgaris occurs spontaneously. The positive value $\Delta H^0$ confirms the endothermic nature of biosorption and the amount of it indicates the physical sorption mechanism. The positive value of $\Delta S^0$ suggests the increased randomness at the interface of solid solution during sorption.

## Adsorption/desorption studies

The used *chlorella vulgaris* biomass was recovered 3 times and showed high stability during 3 adsorption-desorption cycles. The desorption study on the biomass containing thorium ions was conducted using 1 M HCl solution. The results show that the percentage adsorption reduction of thorium ions onto *chlorella vulgaris* decreased only 2.75% in the three cycles. Furthermore, the efficiency of 1 M HCl in the desorption of thorium ions from the biomass decreased from 98.32% in the first cycle to 96.86% in the third cycle. As could be resulted, the thorium ions recovery values are over 96%. According to the obtained results, *chlorella vulgaris* could be regenerated many times with no substantial reduction in metal ion adsorption percentage.

## Conclusion

The obtained results show that the pH and the initial metal ion concentration strongly affect the adsorption capacity of the biosorbent, and the uptake increases with increasing temperature up to 45 °C. The results of the equilibrium study and modeling showed that the Langmuir model is the most suitable isotherm model to describe the biosorption process of thorium ions by *Chlorella vulgaris*. Also, the calculated results using the pseudo-second-order kinetic model are in good agreement with the experimental results. Thermodynamic constants were also evaluated using equilibrium data changing with temperature. The negative value of $\Delta G^0$ indicates spontaneity and the positive values of $\Delta H^0$ and $\Delta S^0$ indicate the endothermic nature and irreversibility of the adsorption process, respectively. The adsorption/desorption studies results showed the *chlorella vulgaris* biosorbent could be regenerated many times with no substantial reduction in metal ion adsorption percentage.

## Data availability

All data generated or analyzed during this study are included in this published article.

Received: 27 January 2024; Accepted: 20 August 2024
Published online: 06 September 2024

## References

1. Degueldre, C. & Joyce, M. J. Evidence and uncertainty for uranium and thorium abundance: A review. *Prog. Nucl. Energy* **124**, 103299 (2020).
2. Zhang, C. *et al.* Zircon Hf-O-Li isotopes of granitoids from the central asian orogenic belt: Implications for supercontinent evolution. *Gondwana Res.* **83**, 132–140 (2020).
3. Zhang, C. *et al.* Hafnium isotopic disequilibrium during sediment melting and assimilation. *Geochem. Perspect. Lett.* **12**, 34–39 (2020).
4. Rhodes, C. J. Current commentary: Thorium-based nuclear power. *Sci. Prog.* **96**(2), 200–209 (2013).
5. Kidd, S. W. *Nuclear fuel resources, in Nuclear Engineering Handbook,* pp. 263–282 (CRC, 2009).
6. Zhang, C. et al. Magmatism and hydrocarbon accumulation in sedimentary basins: A review. *Earth Sci. Rev.* 104531. (2023).
7. Evseeva, T. *et al.* Comparative estimation of 232Th and Stable Ce (III) Toxicity and detoxification pathways in freshwater alga Chlorella vulgaris. *Chemosphere* **81**(10), 1320–1327 (2010).
8. Yarahmadi, A. *et al.* Ce (III) and La (III) ions adsorption through amberlite XAD-7 resin impregnated via CYANEX-272 extractant. *Sci. Rep.* **13**(1), 6930 (2023).
9. Ghorbanpour Khamseh, A. A. *et al.* Intensification of thorium biosorption onto protonated orange peel using the response surface methodology. *Chem. Prod. Process Model.* **18**(4), 657–670 (2023).
10. Leiterer, A., Berard, P. & Menetrier, F. *Thorium and health: State of the art* (2010).
11. Soleymani, F. *et al.* Intensification of strontium (II) ion biosorption on Sargassum Sp via response surface methodology. *Sci. Rep.* **13**(1), 5403 (2023).
12. Khamseh, A. A. G. *et al.* Investigation of kinetic, isotherm and adsorption efficacy of thorium by orange peel immobilized on calcium alginate. *Sci. Rep.* **13**(1), 8393 (2023).
13. Yarahmadi, A. *et al.* Ce (III) and La (III) ions adsorption using amberlite XAD-7 resin impregnated with DEHPA extractant: Response surface methodology, isotherm and kinetic study. *Sci. Rep.* **13**(1), 9959 (2023).
14. Suiyi, Z. *et al.* A novel clinoatacamite route to effectively separate Cu for recycling Ca/Zn/Mn from hazardous smelting waterwork sludge. *J. Environ. Chem. Eng.* **12**(2), 112024 (2024).
15. Heydari, A. *et al.* Configuration Optimization of a renewable hybrid system including biogas generator, photovoltaic panel and wind turbine: Particle swarm optimization and genetic algorithms. *Int. J. Mod. Phys. C* **34**(05), 2350069 (2023).

16. Abdi, S., Nasiri, M. & Khani, M. H. Application of polyaniline nanocomposites in the trapping of thorium ions from aqueous solutions: Adsorption equilibrium, kinetics and thermodynamics. *Prog. Nucl. Energy* **130**, 103537 (2020).
17. Smirnov, A. L. *et al.* Study of scandium and thorium sorption from uranium leach liquors. *J. Radioanal. Nucl. Chem.* **312**, 277–283 (2017).
18. Kütahyalı, C. & Eral, M. Sorption studies of uranium and thorium on activated carbon prepared from olive stones: kinetic and thermodynamic aspects. *J. Nucl. Mater.* **396**(2–3), 251–256 (2010).
19. Bhainsa, K. C. & D'Souza, S. F. Thorium biosorption by aspergillus fumigatus, a filamentous fungal biomass. *J. Hazard. Mater.* **165**(1–3), 670–676 (2009).
20. Keshtkar, A. R. & Hassani, M. A. Biosorption of thorium from aqueous solution by ca-pretreated brown algae cystoseira indica. *Korean J. Chem. Eng.* **31**, 289–295 (2014).
21. Wu, X. *et al.* Sustainable and green sinking electrical discharge machining utilizing foam water as working medium. *J. Clean. Prod.* **452**, 142150 (2024).
22. Kalin, M., Wheeler, W. & Meinrath, G. The removal of uranium from mining waste water using algal/microbial biomass. *J. Environ. Radioact.* **78**(2), 151–177 (2005).
23. Zahiri, M. & Tasharrofi, S. A novel green treatment of groundwater using dead biomass, Schizomeris leibleinii. *Reg. Stud. Mar. Sci.* **45**, 101845 (2021).
24. Du, Y. *et al.* Biodegradation of sulfametoxydiazine by Alcaligenes aquatillis FA: Performance, degradation pathways, and mechanisms. *J. Hazard. Mater.* **452**, 131186 (2023).
25. Ozudogru, Y. & Merdivan, M. Adsorption of U (VI) and th (IV) ions removal from aqueous solutions by pretreatment with Cystoseira barbata. *J. Radioanal. Nucl. Chem.* **323**, 595–603 (2020).
26. Picardo, M. C., de Melo, A. C., Ferreira, & Da Costa, A. C. A. Biosorption of radioactive thorium by Sargassum filipendula. *Appl. Biochem. Biotechnol.* **134**, 193–206 (2006).
27. Bozkurt, S. *et al.* Biosorption of uranium (VI) and thorium (IV) onto Ulva gigantea (Kützing) bliding: Discussion of adsorption isotherms, kinetics and thermodynamic. *J. Radioanal. Nucl. Chem.* **288**(3), 867–874 (2011).
28. Gad, N. S., Samaan, J. M. & Hashem, I. M. Biosorption capacity for uranium and thorium by some microalgae species. *Egypt. J. Microbiol.* **56**(1), 53–60 (2021).
29. Khani, M. & Khamseh, A. G. Statistical analysis, equilibrium and dynamic study on the biosorption of strontium ions on Chlorella vulgaris. *J. Radioanal. Nucl. Chem.* **332**(8), 3325–3334 (2023).
30. Fraile, A. *et al.* Biosorption of copper, zinc, cadmium and nickel by Chlorella vulgaris. *Chem. Ecol.* **21**(1), 61–75 (2005).
31. Vogel, M. *et al.* Biosorption of U (VI) by the green algae Chlorella vulgaris in dependence of pH Value and cell activity. *Sci. Total Environ.* **409**(2), 384–395 (2010).
32. Cheng, J. *et al.* Biosorption capacity and kinetics of cadmium (II) on live and dead Chlorella vulgaris. *J. Appl. Phycol.* **29**, 211–221 (2017).
33. Amini, Y. *et al.* Optimization of liquid–liquid extraction of calcium with a serpentine microfluidic device. *Int. Commun. Heat Mass Transfer* **140**, 106551 (2023).
34. Zarouk, C. *Contribution A l'etude d'une cyanophycee. Influence de divers Facteurs physiques et chimiques sur la croissance et la photosynthese de Spirulina maxinma.* Ph. D. Thesis, Univ. of Paris (1996).
35. Khani, M. Biosorption of strontium by a nonliving brown marine algae, Padina Sp.. *Sep. Sci. Technol.* **47**(13), 1886–1897 (2012).
36. Weber, W. & Morris, J. Advances in water pollution research: removal of biologically resistant pollutants fromwastewaters by adsorption. In *International Conference onWater Pollution Symposium*.
37. Ahmadi-Motlagh, M., Amini, Y. & Karimi-Sabet, J. Experimental study of nitrogen isotope separation by ion-exchange chromatography: Effect of process factors. *J. Radioanal. Nucl. Chem.* **331**(1), 309–315 (2022).
38. Indhumathi, P. *et al.* Utilization, isolation and characterization of chlorella vulgaris for carbon sequestration and waste water treatment by performing FTIR spectral studies. *Asian J. Microbiol. Biotechnol. Environ. Sci.* **15**, 661–666 (2013).
39. Kim, Y. H. *et al.* Removal of lead using xanthated marine brown alga, Undaria Pinnatifida. *Process Biochem.* **34**(6–7), 647–652 (1999).
40. Dean, A., Martin, M. C. & Sigee, D. Resolution of codominant phytoplankton species in a eutrophic lake using synchrotron-based fourier transform infrared spectroscopy. *Phycologia* **46**(2), 151–159 (2007).
41. Baes, C. & Mesmer, R. *The Hydrolysis of Cations*, pp. 177–182 (Wiley, New York, 1976).
42. Tsezos, M. & Volesky, B. The mechanism of uranium biosorption by Rhizopus arrhizus. *Biotechnol. Bioeng.* **24**(2), 385–401 (1982).
43. Huang, Y. *et al.* Selective biosorption of thorium (IV) from aqueous solutions by ginkgo leaf. *PloS One* **13**(3), e0193659 (2018).
44. Zhou, L. *et al.* Biosorption characteristics of uranium (VI) and thorium (IV) ions from aqueous solution using CaCl 2-modified giant kelp biomass. *J. Radioanal. Nucl. Chem.* **307**, 635–644 (2016).
45. Khamseh, A. G. & Ghorbanian, S. A. Experimental and modeling investigation of thorium biosorption by orange peel in a continuous fixed-bed column. *J. Radioanal. Nucl. Chem.* **317**, 871–879 (2018).
46. Elwakeel, K. Z. *et al.* Environmental remediation of thorium (IV) from aqueous medium onto cellulosimicrobium cellulans isolated from radioactive wastewater. *Desalination Water Treat.* **46**(1–3), 1–9 (2012).
47. Albayari, M. et al. Biosorption of uranium (VI) and thorium (IV) from Aqueous solution by marine Sargassum aquifolium macroalgae. *Biomass Convers. Biorefinery* 1–14 (2023).
48. Yang, S. *et al.* Adsorption of thorium (IV) from aqueous solution by non-living biomass of mangrove endophytic fungus Fusarium sp.# ZZF51. *J. Radioanal. Nucl. Chem.* **298**, 827–833 (2013).


## Author contributions

Ke Cheng: wrote the main manuscript text , prepared figures and tables, reviewed the manuscript, Experimental testLingfei Qu: wrote the main manuscript text , prepared figures and tables, reviewed the manuscript, Experimental test Zhiqiang Mao: wrote the main manuscript text , prepared figures and tables, reviewed the manuscript Rong Liao: wrote the main manuscript text , prepared figures and tables, reviewed the manuscript, Experimental testYang Wu: wrote the main manuscript text , prepared figures and tables, reviewed the manuscript Amin Hassanvand: wrote the main manuscript text , prepared figures and tables, reviewed the manuscript.

## Competing interests

The authors declare no competing interests.

## Additional information

**Correspondence** and requests for materials should be addressed to Z.M. or A.H.